Pairing and superfluid properties of dilute fermion gases at unitarity

Vamsi K. Akkineni*
Department of Physics, University of Illinois at Urbana-Champaign, Urbana, Illinois 61801-3080, USA

D. M. Ceperley
NCSA, University of Illinois at Urbana-Champaign, Urbana, Illinois 61801-3080, USA
and Department of Physics, University of Illinois at Urbana-Champaign, Urbana, Illinois 61801-3080, USA

Nandini Trivedi
Department of Physics, The Ohio State University, Columbus, Ohio 43210-1117, USA
(Received 14 September 2007; published 16 October 2007)

We study the system of a dilute gas of fermions in three dimensions, with attractive interactions tuned to the unitarity point, using the nonperturbative restricted path-integral Monte Carlo method. The pairing and superfluid properties of this system are calculated at finite temperature. The total energy at very low temperature from our results agrees closely with that of previous ground-state quantum Monte Carlo calculations. We identify the temperature $T^* \approx 0.70\epsilon_F$, below which pairing correlations develop, and estimate the critical temperature for the superfluid transition $T_c \approx 0.245\epsilon_F$ from a finite size scaling analysis of the superfluid density.

DOI: 10.1103/PhysRevB.76.165116 PACS number(s): 71.27.+a, 05.30.Fk, 02.70.Ss, 03.75.Hh

The recent experiments, starting with generating a degenerate gas of cold atoms,[1] the use of Feshbach resonance to tune the effective interaction between the fermions,[2,3] the measurements of the gap to identify a pairing scale,[4] and the measurements of vortices[5] to identify the superfluid state, have all given an impetus to the study of superfluidity in the BCS Bose-Einstein condensation (BEC) crossover regime.

The nature of superconductivity or superfluidity in a many-particle system with an increasing pairing attraction was shown[6,7] to interpolate smoothly between the BCS regime for weak attraction between the fermions and the BEC regime for strong coupling. In the weak coupling regime, the Cooper pair size is much larger than the interparticle spacing, and the simultaneous pairing and condensation of fermions are well described by the BCS theory. In the strong coupling regime, fermions form strongly bound bosonic molecules at a pairing temperature scale T^* that is considerably higher than the BEC temperature T_c.

In a two species system of fermions with an attractive interaction between them, the unitary point is defined by the divergence of the zero energy s-channel scattering length a_s for two particles in free space. The unitary point is interesting since it describes a strongly correlated system with universal properties.[8] In general, there are two length scales that define the system: the interparticle spacing $\propto n^{-1/3}$ and the scattering length a_s, which contains information about the interaction potential. At the unitary point, however, since a_s diverges, all the properties of the system are described by a single length scale k_F^{-1} or energy scale ϵ_F, where $k_F = (3\pi^2\hbar^3 n)^{1/3}$ is the Fermi momentum of the corresponding noninteracting system.

At the unitarity point, there is no small parameter; therefore, well controlled numerical methods are needed to calculate the properties of the system. Here, we present the first calculation of the superfluid density and other pairing correlations as a function of temperature at the unitary point in a *continuum* model of a two component fermion gas with attractive pairwise interaction between the species. Our main results are (i) an accurate determination of the temperature dependent internal energy which makes it a viable tool for thermometry for cold atoms, (ii) determination of the pairing scale $T^* \simeq 0.7\epsilon_F$ from growth of density correlations of opposite spin fermions, and (iii) determination of the condensation scale $T_c \simeq 0.25\epsilon_F$ from a finite size scaling analysis of the superfluid density. We use the restricted path integral Monte Carlo (R-PIMC) technique, which is the fixed-node extension of the continuum PIMC method to fermionic systems.[9,10] This technique has recently been used to study helium-3, electron-hole liquids, and many body hydrogen.[11]

We consider an unpolarized system of two spins (or two hyperfine species) of particle density n. For the bare two-particle interaction at unitarity, we use the potential (also used in Ref. 14)

$$v(r) = -\frac{2\hbar^2}{m}\frac{\mu^2}{\cosh^2(\mu r)}, \tag{1}$$

where $2/\mu$ is the effective range of the potential. This potential has its only bound state at zero energy, with the eigenfunction given by $\tanh(\mu r)/r$, and a divergent scattering length a_s. We measure distances in units of r_0, the average interparticle spacing, which gives the density $n = 3/(4\pi r_0^3) \simeq 0.238$ and $k_F r_0 = 1.919$. The energy scale is $\epsilon_0 = \hbar^2/mr_0^2$, and the Fermi energy $\epsilon_F = 1.841\epsilon_0$. All the following results were obtained with $\mu r_0 = 12$. In the dilute limit, with the interparticle spacing much larger than the range of the potential $\mu r_0 \gg 1$, the exact form of the potential is unimportant; only the scattering length matters.

Method. For a system of distinguishable quantum particles, the density matrix in configuration space can be written as a path integral over coordinate space variables at discrete imaginary-time intervals as

$$\rho(R_0,R_M;\beta) = \int dR_1 \cdots dR_{M-1} \exp\left[-\sum_{m=1}^{M} S^m\right]. \quad (2)$$

Here, R_m denotes a configuration of $N/2$ up (labeled with $\uparrow$) and $N/2$ down (labeled with $\downarrow$) fermions at the mth time slice. The total extent in the imaginary-time direction, $\beta = 1/k_B T$, is divided into M time slices each of size τ so that $\beta = M\tau$. The link action S^m is the sum of the kinetic-action terms and potential action U^m given by

$$S^m = \frac{3N}{2} \ln(4\pi\lambda\tau) + \frac{(R_m - R_{m-1})^2}{4\lambda\tau} + U^m, \quad (3)$$

with $\lambda = \hbar^2/2m$. Equation (2) is the basis for a quantum-classical isomorphism between a system of quantum particles and a classical system of interacting polymers. Each particle path is interpreted as a polymer, with the beads of the polymer connected with springs described by the kinetic action. The potential action describes the interaction between beads of different polymers.

For indistinguishable quantum particles, the density matrix when evaluated in configuration space requires to be symmetrized for bosons and antisymmetrized for fermions over the particle permutations. For fermions, this antisymmetrized permutation sum is

$$\rho_F(R,R';\beta) = \frac{1}{N!}\sum_{\mathcal{P}} (-1)^{\mathcal{P}} \rho(\mathcal{P}R,R';\beta). \quad (4)$$

In the classical picture, a permutation $\mathcal{P}$ involving n particles corresponds to the cutting and combining of the corresponding n polymers into one large polymer. As paths extend in space at low temperatures, these quantum exchanges become more likely.

For fermions, however, a straightforward evaluation of the fermion density matrix given by Eq. (4) leads to the fermion sign problem. It arises due to the cancellation, at low temperature, of approximately equal contributions from the positive and negative sign permutations, leading to an exponentially vanishing signal-to-noise ratio in the Monte Carlo calculation.[10] In particular, the efficiency of the simulation ξ decreases with particle number N and inverse temperature β as $\xi \propto \exp[-2N(2\pi\lambda\beta)^{3/2}]$.

The R-PIMC method starts from the observation that the path-integral evaluation of the density matrix (4) is the solution to the Bloch equation which governs the imaginary-time evolution of $\rho_F(R,R';\tau)$,

$$-\frac{\partial}{\partial\tau}\rho_F(R,R';\tau) = [-\lambda\nabla_R^2 + V(R)]\rho_F(R,R';\tau). \quad (5)$$

This second order partial differential equation can generally be solved in a region of "space-time" by specifying the initial condition at $\tau=0$ and the boundary conditions for $\tau>0$. The initial condition given by $\rho_F(R,R';0)$ is

$$\rho_F(R,R';0) = \frac{1}{N!}\sum_{\mathcal{P}} (-1)^{\mathcal{P}} \delta(\mathcal{P}R - R'). \quad (6)$$

It can further be shown[10] that it is sufficient to provide the exact boundary conditions on the surface of this region of space-time to obtain the exact solution of the fermion density matrix inside. The density matrix is a function of $2dN+1$ variables (the end configurations and time). To define the region of integration of the Bloch equation, we fix one of the configurations R as the reference point R^* and, for the resulting $dN+1$ dimensioned space-time, choose the initial condition (6) at $\tau=0$ and zero-boundary conditions for all $\tau>0$. Inside this integration region, the solution is given by the usual Boltzmannon path-integral (2). Incorporating the above, the fermion density matrix takes the form[10]

$$\rho_F(R^*,R';\beta) = \int dR_0 \rho_F(R^*,R_0;0) \oint_{R_0\to R' \in \Upsilon_{R^*}} d\{R(\tau)\} e^{-S[\{R(\tau)\}]}. \quad (7)$$

The reach $\Upsilon_{R^*,\tau}$ of R^* is the region of configuration space occupied by boundary-avoiding paths starting from R^* and extending in time to τ. The solution (7) is clearly complicated by the dependence of the reach on $\rho_F(R^*,R;\tau)$, the very quantity we are trying to compute. At any given time τ, the boundaries of the reach, called the nodal surfaces, are complicated $dN-1$ dimensioned hypersurfaces, and not generally known.

To enable the computation, we utilize a trial density matrix constructed to have reasonable physical and topological properties, which defines the nodal surfaces to restrict the paths. The R-PIMC method evades the sign problem for calculations which involve the diagonal elements of the fermion density matrix. Due to the positivity of the density matrix on the diagonal, $\rho_F(R,R;\tau)>0$, we can disregard any paths that start at a negative permutation of R since such paths have to cross a node at least once to end at R. We sum over only the positive (even) permutations and keep only the positive node avoiding paths, thus overcoming the sign problem. The permutation sum, as well as the integrals in Eq. (4), is evaluated with the Metropolis Monte Carlo method.

In the high-temperature limit, it can be shown[12] that the interacting density matrix is well approximated by the free particle density matrix

$$\rho_F(R,R^*;\tau) = (4\pi\lambda\tau)^{-dN/2} \det\left[\exp\left\{\frac{-(\mathbf{r}_i - \mathbf{r}_j^*)^2}{4\lambda\tau}\right\}\right]. \quad (8)$$

In the low-temperature limit, the contributions of the excited states in the spectral expansion of the fermion density matrix,

$$\rho_F(R,R';\tau) = \sum_n \Psi_n(R)\Psi_n^*(R')\exp(-\tau E_n), \quad (9)$$

are exponentially damped relative to the ground state. The density matrix can then be approximated for a nondegenerate ground state as

$$\rho_F(R,R';\tau\to\infty) = \Psi_0(R)\Psi_0^*(R'). \quad (10)$$

For the ground-state trial wave function, we use a BCS-like antisymmetrized product of pairing functions.[13] Denoting the two fermion species with the $\uparrow$ and $\downarrow$ symbols, this trial function is given by

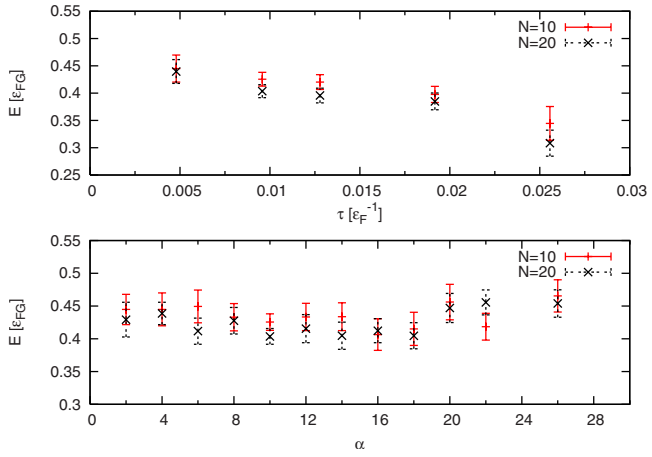

FIG. 1. (Color online) The upper panel shows the energy per particle for $N=10,20$ in units of $\epsilon_{FG}=(3/5)\epsilon_F$ for different choices of the imaginary time step τ. These results obtained for a temperature $T=0.0543\epsilon_F$ indicate that the time step $\tau=0.009\,57\epsilon_F^{-1}$ optimizes the competing requirements of small time step error and efficient computation. The lower panel shows the energy as a function of the parameter α in the pairing function at a temperature of $T=0.0543\epsilon_F$ and time step $\tau=0.009\,57\epsilon_F^{-1}$. The energy has a broad minimum at $\alpha=10-18$, leading to our choice of $\alpha=10$.

$$\Psi_0(R)=\mathcal{A}[\phi(\mathbf{r}_1^{\uparrow}-\mathbf{r}_1^{\downarrow})\phi(\mathbf{r}_2^{\uparrow}-\mathbf{r}_2^{\downarrow})\cdots\phi(\mathbf{r}_{N/2}^{\uparrow}-\mathbf{r}_{N/2}^{\downarrow})]=\det[\phi(\mathbf{r}_i^{\uparrow}-\mathbf{r}_j^{\downarrow})]. \tag{11}$$

The BCS-like trial function allows permutation moves which involve the exchange of a pair of the ↑ and ↓ fermion species with another such pair. Since this is the mechanism for pair condensation in the path-integral formalism, it is important to use this trial function rather than the Slater-Jastrow-type functions which have zero measure for pair exchanges. For the pairing function $\phi(r)$, we choose a Gaussian,

$$\phi(\mathbf{r}_i^{\uparrow}-\mathbf{r}_j^{\downarrow})=\exp[-\alpha(\mathbf{r}_i^{\uparrow}-\mathbf{r}_j^{\downarrow})^2], \tag{12}$$

with α the one free parameter to be optimized.

Results. In discussing the results, we give temperature T in units of the Fermi energy ϵ_F and energy in units of ϵ_{FG}, the average energy per particle of the noninteracting Fermi gas, with $\epsilon_{FG}=(3/5)\epsilon_F$. For a given observable, the length of the discrete time interval τ in Eq. (2) results in a time-step error due to the nonexact link action used. The time step also affects the statistical error of the observable by affecting the efficiency of Monte Carlo sampling.[9] In general, both the time step error and the efficiency decrease with τ so that it is important to choose a time step that satisfies these competing considerations. We use the total energy as the observable, and Fig. 1 shows the energy for different τ at temperature $T=0.0543\epsilon_F$. We choose the time step $\tau=0.009\,57\epsilon_F^{-1}$ (with $M=1920$ time slices) since it is in a range where the change in energy estimate with τ is within the statistical error and also allows for efficient calculation.

The R-PIMC method obeys a variational principle that the free energy calculated at any temperature is a functional of the trial density matrix nodes and is minimized when the trial nodes coincide with those of the exact density matrix. This minimum value is also the true free energy of the given Hamiltonian. At very low temperatures, the thermodynamic relation $F=E-TS$ allows us to use the energy E to improve the nodal surfaces. For the trial function (11), we optimize the parameter α which controls the width of the Gaussian pairing function (12). The lower panel of Fig. 1 shows the energy for different α at $T=0.0543\epsilon_F$ with time step $\tau=0.009\,57\epsilon_F^{-1}$. The energy has a rather broad minimum for $\alpha=10-18$, leading to our choice of $\alpha=10$.

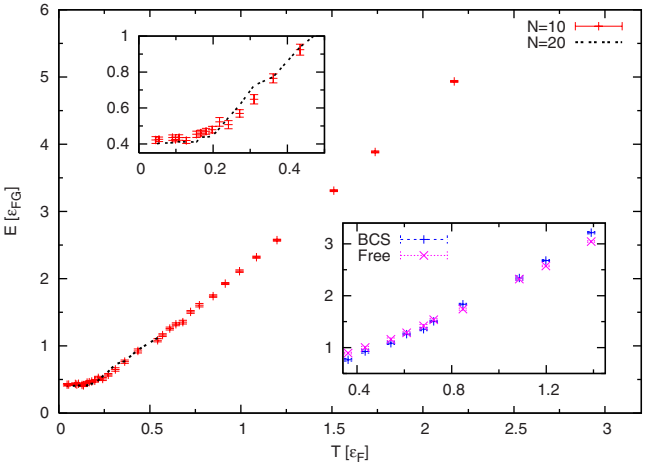

FIG. 2. (Color online) The energy per particle as a function of T for $N=10$ and 20 (dashed line; error bars not shown but comparable to $N=10$.) The upper inset magnifies the energy at low temperature, obtained using the BCS-like nodes. The lower inset shows the energy for $N=10$ in the temperature region where the lowest energy is obtained by changing from free-fermion nodes ("Free") to the BCS-like nodes ("BCS").

The total energy vs temperature is shown in Fig. 2 for $N=10$ and $N=20$. The BCS-like trial density matrix, in addition to its enabling the physics of pairing and condensation, is further justified because it gives the lowest total energy at low temperature of all the trial density matrices that we have tested. We also find good agreement of our energy extrapolated to $T=0$ with the value of $E_o/N=0.44(1)\epsilon_{FG}=0.26\epsilon_F$ obtained from the fixed-node Green's function Monte Carlo method.[14,15]

We can further calculate the quasiparticle energy as the energy difference between a system with an extra particle of one species and a system with equal number of particles of the two species. Taking N to be an even number so that there are $N/2$ pairs in the system, the energy gap is obtained as

$$\Delta E=(N+1)\epsilon_{N+1}-\frac{1}{2}[N\epsilon_N+(N+2)\epsilon_{N+2}], \tag{13}$$

where ϵ_N, ϵ_{N+1}, and ϵ_{N+2} are the energy per particle of systems with N, $N+1$, and $N+2$ particles, respectively. The trial density matrix for the system with $N+1$ particles is constructed from antisymmetrized trial wave functions with $N/2$ pair states and one extra particle in a plane-wave state given by

TABLE I. Calculation of the quasiparticle energy gap with different trial functions.

N	k_n (k_F)	ϵ_N (ϵ_{FG})	ΔE (ϵ_{FG})
10		0.425 (0.0125)	
11	0	0.615 (0.0155)	2.111 (0.1973)
11	0, 0.913	0.528 (0.0138)	1.155 (0.1812)
11	0.913	0.543 (0.0127)	1.315 (0.1717)
11	0, 0.913, 1.291	0.524 (0.0133)	1.110 (0.1766)
11	1.291	0.592 (0.0139)	1.861 (0.1823)
12		0.421 (0.0126)	
20		0.403 (0.0119)	
21	0, 0.736	0.460 (0.0126)	1.058 (0.3383)
21	0, 0.736, 1.041	0.436 (0.0137)	0.538 (0.3568)
22		0.416 (0.0157)	

$$\Psi_n(R) = \mathcal{A}[\phi(\mathbf{r}_1^{\uparrow} - \mathbf{r}_1^{\downarrow}) \cdots \phi(\mathbf{r}_{N/2}^{\uparrow} - \mathbf{r}_{N/2}^{\downarrow}) \exp(-i\mathbf{k}_n \cdot \mathbf{r}_{N/2+1}^{\uparrow})]. \tag{14}$$

These trial functions are used in the spectral expansion (9) to obtain the trial density matrix for this system. Table I shows the quasiparticle energy calculated at a temperature $T = 0.0543\epsilon_F$ with $N=10$ and $N=20$. The second column shows the momentum of the plane-wave states of the extra particle in systems of size $N+1$. These states correspond to the lowest momentum shells of the system with periodic boundaries. The lowest value of the energy gap is obtained when the extra particle is allowed to occupy the first three momentum shells in the trial density matrix. With $N=20$ and larger system sizes, the error bar of the energy gap is rather large. At $N=10$, however, our value of $\Delta E = 1.110(0.1766)\epsilon_{FG}$ agrees with the value of $\Delta E = 0.9\epsilon_{FG}$ from earlier GFMC calculations.[14]

Estimation of T_c. The first indication of the crossover pairing scale $T^* \approx 0.70\epsilon_F$ is obtained from a comparison of the energy obtained by using the free particle trial density matrix and the BCS-like density matrix as shown in Fig. 2. For $T \geqslant T^*$, the free particle density matrix gives the lowest energy, whereas in the opposite regime $T \leqslant T^*$, the BCS density matrix gives the lowest energy.

Further evidence of the pairing scale comes from $g_{\uparrow\text{-}\downarrow}$ pairing correlations as seen in Fig. 3. As the temperature is lowered, there is a strong enhancement of the on-site density correlations for opposite spins at $T \sim 0.67\epsilon_F$ (see inset), which identifies a pairing scale below which strong pairing correlations exist at temperatures well above the actual superfluid transition.

In previous work,[16] a functional integral approach was used to estimate T^* as a function of $1/(k_F a_s)$ from a saddle point analysis of the gap and number equations. At unitarity, they found $T^* \simeq 0.57\epsilon_F$. Upon including fluctuations to quadratic order around the saddle point, the transition was suppressed, especially around unitarity and beyond, to a lower T_c. They estimated $T_c \simeq 0.22\epsilon_F$ at unitarity. The inclusion of the fluctuations around the saddle point to fourth order

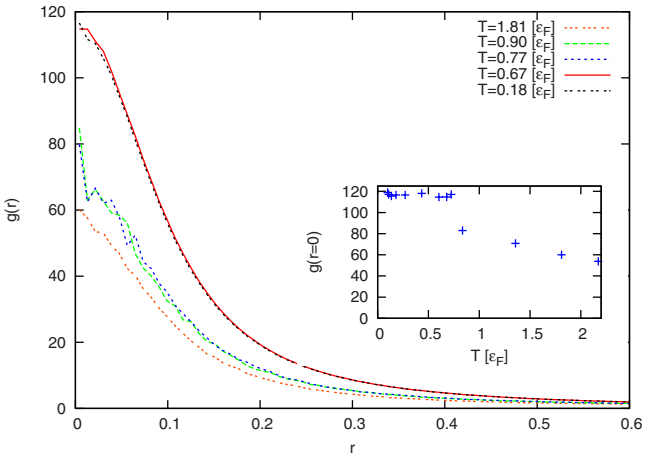

FIG. 3. (Color online) The pair correlation function of the two species of fermions at different values T. Note the sharp increase in pair correlation from $0.67T_F$ to $0.54T_F$.

showed that the variations of T_c are controlled by the coherence length $k_F\xi_0$. In the BCS regime, $k_F\xi_0$ is exponentially large, while in the BEC regime, for a dilute Bose gas, $k_F\xi_0$ grows as a power law. In both these regimes, T_c variations are small. However, around the unitary point, $k_F\xi_0 \sim \mathcal{O}(1)$ and the fluctuations in T_c/ϵ_F are of order unity. This is precisely where simulations are of greatest value since the system is in a strongly correlated regime inaccessible to perturbation theory.

We compute the superfluid density to directly estimate the critical temperature T_c for the superfluid transition. The superfluid density ρ_s for an N-particle system, shown Fig. 4, is calculated from the winding number estimator,[17]

$$\frac{\rho_s}{\rho} = \frac{\langle \mathbf{W}^2 \rangle}{2\lambda\beta N}. \tag{15}$$

Here, $\mathbf{W}$ is the winding number defined as the number of times periodic boundary conditions are invoked as paths start from R_i and end at a periodic image $R_{\mathcal{P}i}$. For our system, the

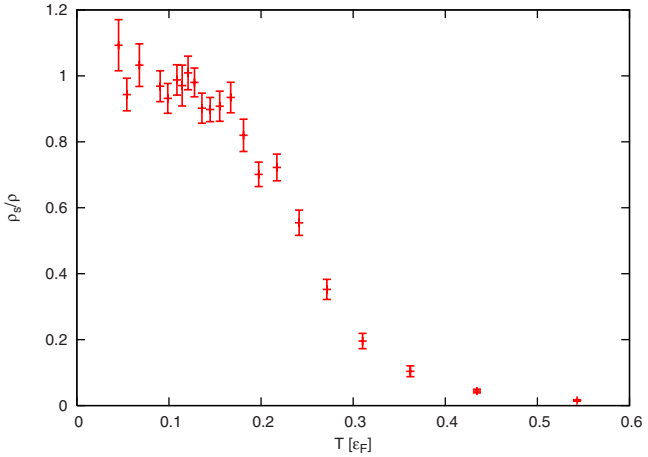

FIG. 4. (Color online) The superfluid fraction ρ_s/ρ as a function of T for $N=20$.

winding number is given by $\mathbf{W}=\mathbf{W}_{\uparrow}+\mathbf{W}_{\downarrow}$. The estimator (15) for the superfluid density might, however, be biased by the fixed-node approximation. The winding number estimator is the integration over imaginary time of the momentum-momentum correlation, but observables are only unbiased at the reference point (the zero of imaginary time): the time slice that defines the nodal region. It is not known how this bias will affect the calculation of the critical properties.

We start by reviewing the Josephson relation which is a hyperscaling relation between the correlation length exponent ν defined by $\xi \sim t^{-\nu}$ and the superfluid density exponent ζ defined by $\rho_s \sim t^{\zeta}$, where $t=(T-T_c)/T_c$ is the reduced temperature. The singular part of the free energy density near the transition is $f_s(t) \sim \xi^{-d}$, and since $\rho_s(\nabla\phi)^2 \sim f_s$, we obtain $\rho_s \sim \xi^{-(d-2)} \sim t^{\nu(d-2)}$, which directly gives the Josephson relation[18] $\zeta/\nu=d-2$. In a finite system, the scaling hypothesis[18] $f_s(t,L)=L^{-d}\mathcal{F}[L/\xi(t)]$ states that the free energy depends on t only through the ratio of the system size L and the bulk correlation length ξ. Using the Josephson relation, this implies that $\rho_s(t,L)=L^{2-d}Q[L/\xi(t)]$. In $d=3$, linearizing the function Q near $t=0$ and using $L \sim N^{1/3}$ lead to

$$Q\left[\frac{L}{\xi(t)}\right] = N^{1/3}\frac{\rho_S(t)}{\rho} \approx Q(0) + qN^{1/3\nu}\frac{T-T_c}{T_c}, \qquad (16)$$

where q is a constant. In Fig. 5, we plot $N^{1/3}\rho_s(t)/\rho$ vs T for several system sizes N. At the transition temperature T_c, the size dependence vanishes and all the curves meet at a point which determines the critical temperature $T_c \approx 0.255\epsilon_F$. Our result agrees well with the estimate of $T_c \approx 0.22\epsilon_F$ (Ref. 16) obtained by including fluctuations around the saddle point.

The transition temperature has also been calculated using lattice Monte Carlo techniques.[19,20] Our estimate is, however, higher than the lattice Monte Carlo estimate of Burovski *et al.* of $T_c \approx 0.15\epsilon_F$.[20] The main distinction of our path-integral Monte Carlo is that we work directly in the continuum so the unitary limit is perfectly well defined. The lattice simulations have to extrapolate T_c to the zero filling factor limit in order to get the correct behavior in the unitary limit. On the other hand, for the attractive-U Hubbard model, there is no sign problem,[21] which is a definite advantage. However, given the good agreement of our finite temperature R-PIMC method with the zero temperature GFMC results for the energy, we believe we have an accurate description of the nodal surface. The R-PIMC method can further be used to study the competition between superfluidity and magnetization in unequal fermion populations.

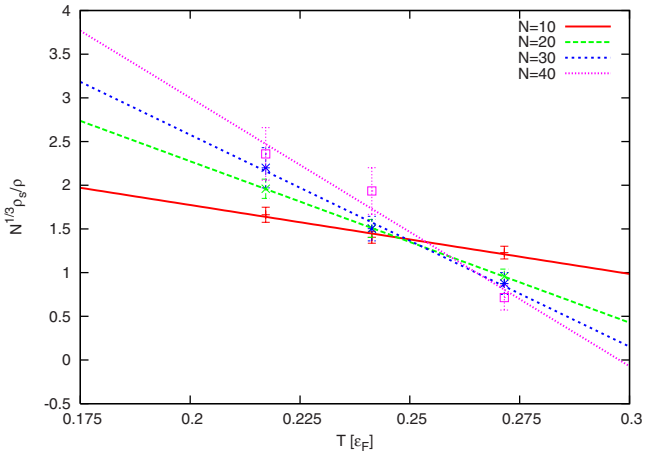

FIG. 5. (Color online) The scaled, linearized, superfluid density $N^{1/3}\rho_s/\rho$ as a function of T for $N=10$, 20, 30, and 40. The intersection of the four lines gives the superfluid transition temperature as $T_c \approx 0.255T_F$.

One of the difficulties in the experiments is determining the temperature precisely. Usually, a Maxwell-Boltzmann fit to the excited atoms yields an estimate. However, at low temperatures when the number of atoms in the excited states is greatly reduced, such an estimate becomes unreliable.[22] The strong dependence of the energy on temperature above T_c seen from our results indicates that measurements of the mean field energy can be converted to a temperature scale, with appropriate corrections for a trap using a local density approximation.

We would like to thank Mohit Randeria, Roberto Diener, and Jason Ho for valuable discussions. This work has been supported by the NSF under the Grant No. DMR-0404853. Computer time was provided by the Materials Computation Center at the University of Illinois at Urbana-Champaign.

*akkineni@uiuc.edu

[1] B. DeMarco and D. S. Jin, Science **285**, 1703 (1999); A. G. Truscott, K. E. Strecker, W. I. McAlexander, G. B. Partridge, and R. G. Hulet, *ibid.* **291**, 2570 (2001).

[2] C. A. Regal, C. Ticknor, J. L. Bohn, and D. S. Jin, Nature (London) **424**, 47 (2003); M. Greiner, C. A. Regal, and D. S. Jin, *ibid.* **426**, 537 (2003).

[3] S. Gupta, Z. Hadzibabic, M. W. Zwierlein, C. A. Stan, K. Dieckmann, C. H. Schunck, E. G. M. van Kempen, B. J. Verhaar, and W. Ketterle, Science **300**, 1723 (2003); T. Bourdel, J. Cubizolles, L. Khaykovich, K. M. F. Magalhães, S. J. J. M. F. Kokkelmans, G. V. Shlyapnikov, and C. Salomon, Phys. Rev. Lett. **91**, 020402 (2003).

[4] C. Chin *et al.*, Science **305**, 1128 (2004).

[5] M. W. Zwierlein, J. R. Abo-Shaeer, A. Schirotzek, C. H. Schunck, and W. Ketterle, Nature (London) **435**, 1047 (2005).

[6] D. R. Eagles, Phys. Rev. **186**, 456 (1969); A. J. Leggett, in *Modern Trends in the Theory of Condensed Matter*, edited by A. Pekalsky and R. Przystawa (Springer-Verlag, Berlin, 1980); J. Phys. (Paris), Colloq. **41**, C7-19 (1980).

[7] M. Randeria, in *Bose Einstein Condensation*, edited by A. Griffin, D. W. Snoke, and S. Stringari (Cambridge, New York, 1995), pp. 355–392.

[8] T. L. Ho, Phys. Rev. Lett. **92**, 090402 (2004).

[9] D. M. Ceperley, Rev. Mod. Phys. **67**, 279 (1995).

[10] D. M. Ceperley, in *Monte Carlo and Molecular Dynamics of*

Condensed Matter Systems, edited by K. Binder and G. Ciccotti (Editrice Compositori, Bologna, Italy, 1996); J. Shumway and D. M. Ceperley, Proceedings of the 1999 International Conference on Strongly Coupled Coulomb Systems, Saint-Malo, France (unpublished).

[11] D. M. Ceperley, Phys. Rev. Lett. **69**, 331 (1992); M. Boninsegni and D. M. Ceperley, *ibid.* **74**, 2288 (1995); C. Pierleoni, D. M. Ceperley, B. Bernu, and W. R. Magro, *ibid.* **73**, 2145 (1994); W. R. Magro, D. M. Ceperley, C. Pierleoni, and B. Bernu, *ibid.* **76**, 1240 (1996); B. Militzer and D. M. Ceperley, *ibid.* **85**, 1890 (2000); Phys. Rev. E **63**, 066404 (2001).

[12] D. M. Ceperley, J. Stat. Phys. **63**, 1237 (1991); L. Mitas, arXiv:cond-mat/0601485 (unpublished); arXiv:cond-mat/0605550 (unpublished).

[13] For the pairing function $\phi(\mathbf{r}_i^{\uparrow} - \mathbf{r}_j^{\downarrow})$, we choose a Gaussian with one free parameter that is optimized; the results are not sensitive to this specific choice.

[14] J. Carlson, S.-Y. Chang, V. R. Pandharipande, and K. E. Schmidt, Phys. Rev. Lett. **91**, 050401 (2003); S.-Y. Chang, V. R. Pandharipande, J. Carlson, and K. E. Schmidt, Phys. Rev. A **70**, 043602 (2004).

[15] G. E. Astrakharchik, J. Boronat, J. Casulleras, and S. Giorgini, Phys. Rev. Lett. **93**, 200404 (2004).

[16] C. A. R. Sa de Melo, M. Randeria, and J. R. Engelbrecht, Phys. Rev. Lett. **71**, 3202 (1993).

[17] E. L. Pollock and D. M. Ceperley, Phys. Rev. B **36**, 8343 (1987).

[18] N. Goldenfeld, *Lectures on Phase Transitions and the Renormalization Group* (Addison-Wesley, Reading, MA, 1992).

[19] A. Bulgac, J. E. Drut, and P. Magierski, Phys. Rev. Lett. **96**, 090404 (2006).

[20] E. Burovski, N. Prokof'ev, B. Svistunov, and M. Troyer, Phys. Rev. Lett. **96**, 160402 (2006).

[21] M. Randeria, N. Trivedi, A. Moreo, and R. T. Scalettar, Phys. Rev. Lett. **69**, 2001 (1992); N. Trivedi and M. Randeria, *ibid.* **75**, 312 (1995).

[22] J. Kinast, A. Turlapov, J. E. Thomas, Q. Chen, J. Stajic, and K. Levin, Science **307**, 1296 (2005).